The Shwachman-Bodian-Diamond syndrome gene encodes an RNA-binding protein that localizes to the pseudopod of *Dictyostelium* amoebae during chemotaxis

Deborah Wessels[1], Thyagarajan Srikantha[1], Song Yi[1], Spencer Kuhl[1], L. Aravind[2] and David R. Soll[1,*]

[1]W.M. Keck Dynamic Image Analysis Facility, Department of Biological Sciences, The University of Iowa, Iowa City, IA 52242, USA
[2]Computational Biology Branch, NCBI, NLM, NIH, Bethesda, MD 20894, USA
*Author for correspondence (e-mail: david-soll@uiowa.edu)

Accepted 24 October 2005
Journal of Cell Science 119, 370-379 Published by The Company of Biologists 2006
doi:10.1242/jcs.02753

Summary

The Shwachman-Bodian-Diamond syndrome (SBDS) is an autosomal disorder with multisystem defects. The Shwachman-Bodian-Diamond syndrome gene (*SBDS*), which contains mutations in a majority of SBDS patients, encodes a protein of unknown function, although it has been strongly implicated in RNA metabolism. There is also some evidence that it interacts with molecules that regulate cytoskeletal organization. Recently, it has been demonstrated by computer-assisted methods that the single behavioral defect of polymorphonuclear leukocytes (PMNs) of SBDS patients is the incapacity to orient correctly in a spatial gradient of chemoattractant. We considered using the social amoeba *Dictyostelium discoideum*, a model for PMN chemotaxis, an excellent system for elucidating the function of the SBDS protein. We first identified the homolog of *SBDS* in *D. discoideum* and found that the amino acids that are altered in human disease were conserved. Given that several proteins involved in chemotactic orientation localize to the pseudopods of cells undergoing chemotaxis, we tested whether the *SBDS* gene product did the same. We produced an *SBDS-GFP* chimeric in-frame fusion gene, and generated transformants either with multiple ectopic insertions of the fusion gene or multiple copies of a non-integrated plasmid carrying the fusion gene. In both cases, the SBDS-GFP protein was dispersed equally through the cytoplasm and pseudopods of cells migrating in buffer. However, we observed differential enrichment of SBDS in the pseudopods of cells treated with the chemoattractant cAMP, suggesting that the SBDS protein may play a role in chemotaxis. In light of these results, we discuss how SBDS might function during chemotaxis.

Supplementary material available online at
http://jcs.biologists.org/cgi/content/full/119/2/370/DC1

Key words: Computer-assisted motion analysis, *SBDS* gene, Pseudopod localization, CAMP chemoattractant

Introduction

The Shwachman-Bodian-Diamond Syndrome (SDS) is an autosomal disorder with multisystem defects that can include pancreatic insufficiency, skeletal abnormalities, bone marrow dysfunction, immune deficiency and, in some cases, leukemic transformation (Shwachman et al., 1964; Bodian et al., 1964; Ginzberg et al., 1999; Mack et al., 1996; Cipolli, 1999; Makitie et al., 2004). SBDS patients frequently are neutropenic and suffer from chronic infections, but even when they are not neutropenic, they are prone to infection, suggesting white blood cell defects (Aggett et al., 1980; Dror et al., 2001). Earlier observations, using primarily transmembrane assays, suggested white blood cell abnormalities in motility and/or chemotaxis (Aggett et al., 1980; Dror et al., 2001; Repo et al., 1987; Ruuter et al., 1984). Recent computer-assisted analysis of the individual behavior of polymorphonuclear leukocytes (PMNs) of SDS patients demonstrated a single chemotactic defect. Although the PMNs of SBDS patients migrated normally in buffer, responded normally to the temporal dynamics of simulated temporal waves of chemoattractant and exhibited a chemokinetic response to chemoattractant, they were unable to orient correctly in spatial gradients of chemoattractant (Stepanovic et al., 2004). In a spatial gradient of chemoattractant locomotion was normal but direction was random. Based on these observations, we hypothesized that the PMNs of SBDS patients are defective in a component of the machinery that regulates orientation in a spatial gradient of chemoattractant. Such components often distribute to the anterior end of a cell undergoing chemotaxis (Postma et al., 2004; Van Haastert et al., 2004). However, this hypothesis seemed inconsistent with the deduced function of the protein encoded by the Shwachman-Bodian-Diamond Syndrome gene (*SBDS*), which is mutated in a majority (75-89%) of SBDS patients (Boocock et al., 2003; Kuijper et al., 2005). The major mechanism for mutations appears to be a gene-conversion event between the SBDS gene and a pseudogene (Boocock et al., 2003; Nakashima et al., 2004).

Structural, biochemical and genetic studies indicated that the SBDS protein is involved in RNA metabolism (processing or transport) (Savchenko et al., 2005), and immunofluorescent

Journal of Cell Science

Journal of Cell Science

studies revealed that, although distributed throughout the cytoplasm, there was increased localization in the nucleoli of fibroblasts and lymphocytes (Austin et al., 2005). These latter results were consistent with a general role for the SBDS protein in RNA metabolism, but they did not seem to be consistent with the very selective chemotactic defect exhibited by SBDS PMNs (Stepanovic et al., 2004). There were, however, alternative explanations for a role for *SBDS* in the selective defect in the chemotactic orientation of PMNs and SBDS patients. First, it has been demonstrated that β-actin mRNA localizes to the leading edge of cells for the assembly of β-actin-specific compartments (Sundell and Singer, 1990; Hill and Gunning, 1993; Kislauskis et al., 1994; Condeelis and Singer, 2005). In addition, Mingle et al. (Mingle et al., 2005) demonstrated that serum stimulates the localization of the mRNAs of the seven major proteins of the Arp2/3 complex in fibroblast protrusions, suggesting that localized translation regulates cellular protrusions. In addition, the gene product of the yeast homolog of SBDS, YLR022C, has been shown to bind strongly to liposomes tagged with phosphinositide (Zhu et al., 2001), an intracellular signaling molecule, which plays a major role in chemotaxis (Maffucci and Falasca, 2001; Funamoto et al., 2001). YLR022C has also been shown to interact with Rho3p (Ito et al., 2001), a GTPase involved in actin organization (Rivero and Somesh, 2002; Zohn et al., 1998). Therefore, we considered the possibilities that SBDS either plays a role in the transport and localization of transcripts encoding proteins involved in chemotactically induced polarization or participates directly in the reorganization of the actin cytoskeleton during attractant-induced polarization.

Given three alternative possibilities, we decided to test whether the SBDS protein localized to the leading edge of a cell oriented in a spatial gradient of chemoattractant by using the soil amoeba *D. discoideum* (Soll et al., 2002; Parent, 2004; Devreotes and Janetopoulos, 2003; Geiger et al., 2003). The behavior of *Dictyostelium* amoebae perfused with buffer, challenged with a spatial gradient of chemoattractant or treated with temporal gradients of chemoattractant, is remarkably similar to that of human polymorphonuclear leukocytes (Geiger et al., 2003). Because *Dictyostelium* is haploid, gene disruption or replacement is readily accomplished (Kuspa and Loomis, 1994; Kessin, 2001). An SBDS homolog is present as a single copy in the *Dictyostelium* genome (Shammas et al., 2005). Furthermore, the most common bases found mutated in the gene of SBDS patients (Boocock et al., 2003) are conserved in the *D. discoideum* homolog. To test whether the SBDS protein localizes to the anterior pseudopod during chemotaxis, we overexpressed green fluorescent protein (GFP)-tagged SBDS in *D. discoideum* and analyzed the distribution of SBDS-GFP in amoebae migrating in buffer in the absence of a chemoattractant, or undergoing chemotaxis in a spatial gradient of chemoattractant. Whereas the SBDS protein remained equally dispersed throughout the cytoplasm of the cell body and pseudopods of cells migrating in buffer, it enriched in the anterior pseudopod of cells undergoing chemotaxis in a spatial gradient of chemoattractant. It also localized to the sites from which new lateral pseudopods formed in cells undergoing chemotaxis. These results indicate that the SBDS protein enriches in the pseudopods of cells sensing a spatial gradient of chemoattractant. In *Dictyostelium*, several molecules involved in the regulation of chemotaxis localize in pseudopods (Postma et al., 2004; Van Haastert and Devreotes, 2004), including the pleckstrin homology (PH)-domain-containing protein CRAC (Parent et al., 1998), the G protein βγ complex (Jin et al., 2000), protein kinase B (Akt/PKB) (Meili et al., 1999; Chung et al., 2001), the Arp2/3 complex (Insall et al., 2001) and PI 3 kinase (Funamoto et al., 2002). Similar molecules localize to the pseudopodia of human neutrophils (Servant et al., 2000) and fibroblasts (Haugh et al., 2000). The chemoattractant-induced enrichment pattern of SBDS is unique for a protein with deduced functions in ribosome metabolism, RNA transit from the nucleus and RNP processing, and may be related to interactions with the actin cytoskeleton inferred from suggested interactions of the yeast SBDS homolog with phosphinositides and Rho3p (Zhu et al., 2001).

Results

The *D. discoideum* SBDS protein

The SBDS protein is conserved in organisms throughout the archaeal and eukaryotic superkingdoms, but is absent in eubacteria (Shammas et al., 2005). The annotated coding sequence DDB0206557 of *D. discoideum* (http://dictybase.org/), the ortholog of the human SBDS, encodes a protein containing 274 amino-acid residues, compared to 250 amino acids in the human protein (Fig. 1). The difference in size is due to a unique 24 amino acid tail at the C-terminus of the *Dictyostelium* SBDS (Fig. 1). The *D. discoideum* SBDS protein exhibits an overall identity of 38% and similarity of 69% with the human ortholog. As previously revealed in an analysis of the primary sequence and secondary structure, the *D. discoideum* and human SBDS proteins

Fig. 1. Alignment of human and *D. discoideum* SBDS proteins. The boundaries of the three major domains in SBDS and related orthologs include: an N-terminal module with two motifs, SHHP1 and SHHP2; a central tri-helical bundle module; and a C-terminal module with RNA-recognition motif (RRM-like). The four β strands (E-runs) and four helices (H-runs) in the N-terminal module, and the unique 24-residue tail of the *Dictyostelium* SBDS ortholog are indicated.

Journal of Cell Science

(Shammas et al., 2005) contain three conserved modules (Fig. 1): (1) an N-terminal module with four β strands (E-runs) and four helices (H-runs), (2) a central domain forming a tri-helical bundle with a fold associated with DNA-binding (tri-helical bundle), and (3) a C-terminal domain, with a fold associated with RNA-recognition (RRM-like). Our comparative analysis of the N-terminal module of the *D. discoideum* SBDS protein, based on the 3D structures of the *S. cerevisiae* SBDS homolog Yhr087w and the *Archaeoglobus* SBDS homolog AF0491, revealed that it is comprised of a dyad repeat of a simple structural motif, not previously resolved. Each of these structural motifs is comprised of a two-β-strand hairpin followed by a two-α-helix hairpin, which we have named the strand-helix-hairpin (SHHP) motif. These two SHHP motifs are placed orthogonally to each other, forming a prominent cleft that might serve as a surface for interactions with a ribonucleoprotein complex. Interestingly, five of the original eight mutations associated with SBDS in humans (Boocock et al., 2003) map to the first SHHP motif and three to the second SHHP motif (Fig. 1). The majority of the amino acids originally found to be altered in SBDS patients (Boocock et al., 2003) are conserved in *D. discoideum* (Fig. 1).

Transformants containing ectopically integrated copies of *SBDS-GFP*

The *D. discoideum* SBDS ortholog was cloned by PCR amplification. To generate an in-frame fusion with GFP, a GFP-neomycin expression module that confers G418 resistance (Levi et al., 2000) was introduced at the 5′ end of the TAA stop codon of *D. discoideum SBDS* by inverse PCR. Cells of strains AX2 and AX3 were transformed by electroporation with the linear fragment containing the neomycin-resistance gene and the *SBDS-GFP* fusion, and resulting transformants were selected for G418 resistance. The integrity of the *SBDS-GFP* cassette was verified in four GFP-expressing AX3 clones and one GFP-expressing AX2 clone by PCR and sequencing of the PCR products. The transformants AX3p2.1.2 and AX2p2.3.1 were chosen for fluorescent analysis. Quantitative analysis of Southern blots probed with the *SBDS* gene indicated that both strains contained between 15 and 20 copies of the cassette integrated ectopically (data not shown). Quantitative northern blots probed with the *SBDS* gene indicated that the level of *SBDS-GFP* transcript was 15 to 20 times that of the endogenous *SBDS* gene transcript (Fig. 2).

Distribution of the SBDS protein in the absence of attractant

Cells of both transformants AX3p2.1.2 and AX2p2.3.1 migrating in buffer in the absence of chemoattractant were motion analyzed with the DIAS motion analysis software program (Soll, 1995; Soll and Voss, 1998) for shape parameters, velocity, directional change and pseudopod dynamics. The behavior of the transformants was indistinguishable from that of parental control cell lines (data not shown). We therefore conclude that overexpression of *SBDS-GFP* has no effect on cell behavior.

Laser scanning confocal microscopy (LSCM) of cells in buffer, imaged 1 μm above the substratum, revealed that *SBDS-GFP* was distributed equally throughout the cytoplasm (Fig. 4A-C; supplementary material Movie 1, panel A; Movie 2, panel A), including the particulate cytoplasm of the main cell body and the non-particulate cytoplasm of the pseudopod (Fig. 3A-C). There was no enrichment in the cell cortex, pseudopod or uropod. This held true for LSCM scans through the entire *z*-axis of each cell (data not shown), and over a 50-second time series of a migrating cell imaged at short time intervals 1 μm above the substratum (Fig. 3D).

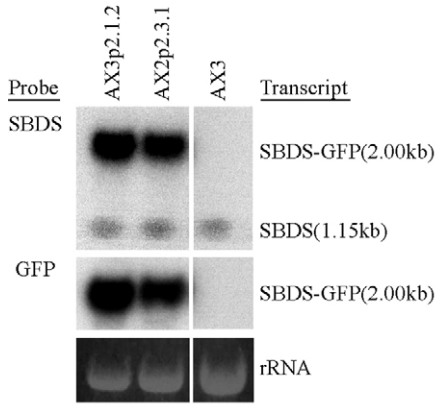

Fig. 2. Northern analysis of *SBDS-GFP* using the *GFP* and the *SBDS* sequences as probes.

To quantitate the distribution of label along the anterior-posterior cell axis, we computed the average pixel intensity along line scans through different regions of LSCM images (Fig. 4A) of cells migrating in buffer over a 150-second period. Line scans were made 1 μm above the substratum. For the four analyzed cells, average pixel intensity across the anterior pseudopod, the anterior portion of the cell body and the posterior portion of the cell body were similar and remained constant over the 150-second period of analysis (Fig. 4B-E). Scans of lateral pseudopods computed for one cell also did not reveal differential localization (Fig. 4B). The ratio of average intensity across the anterior pseudopod versus cell body (in this case halfway along the length of the cell) for nine amoebae (each averaged over 50 frames during a 150-second period) was 1.07±0.14 (Table 1), supporting the interpretation that there is little localization of the SBDS-GFP protein during cell migration in buffer.

Table 1. The ratio of pixel intensity of pseudopod to cell body, of cells migrating in buffer and cells migrating in a spatial gradient of chemoattractant

Buffer (absence of cAMP)		Spatial gradient of cAMP	
Cell number	Intensity ratio (pseudopod:cell body)	Cell number	Intensity ratio (pseudopod:cell body)
1	1.14	1	1.42
2	1.19	2	2.07
3	0.84	3	1.32
4	1.28	4	1.68
5	1.05	5	1.21
6	1.01	6	1.33
7	0.98	7	1.45
8	1.18	8	1.37
9	0.96	9	1.65
Mean ± s.d.	1.07±0.14		1.50±0.26

P=0.0033.

Distribution of the SBDS protein during chemotaxis

Like amoebae migrating in buffer, amoebae undergoing chemotaxis are polarized, with a dominant anterior pseudopod and identifiable posterior uropod. On average, they are more elongate than cells in buffer, and form lateral pseudopods far less frequently (Varnum-Finney et al., 1987a; Varnum-Finney et al., 1987b; Stepanovic et al., 2005). In a spatial gradient of chemoattractant, the majority of migrating cells are oriented in the direction of increasing chemoattractant concentration. Cells of both transformants AX3p2.1.2 and AX2p2.3.1 undergoing chemotaxis in spatial gradients of chemoattractant were analyzed with DIAS motion analysis software (Soll, 1995; Soll and Voss, 1998) for shape parameters, velocity, directional change, pseudopod dynamics, chemotactic index and percent positive chemotaxis. The chemotactic behavior of the transformants was indistinguishable from that of parental control cell lines (data not shown).

LSCM scans of these cells, 1 μm above the substratum, revealed a distribution different from that of cells migrating in buffer. These cells were imaged at the same LSCM settings used to image cells migrating in buffer. Although distributed throughout the cell, the level of SBDS-GFP was consistently

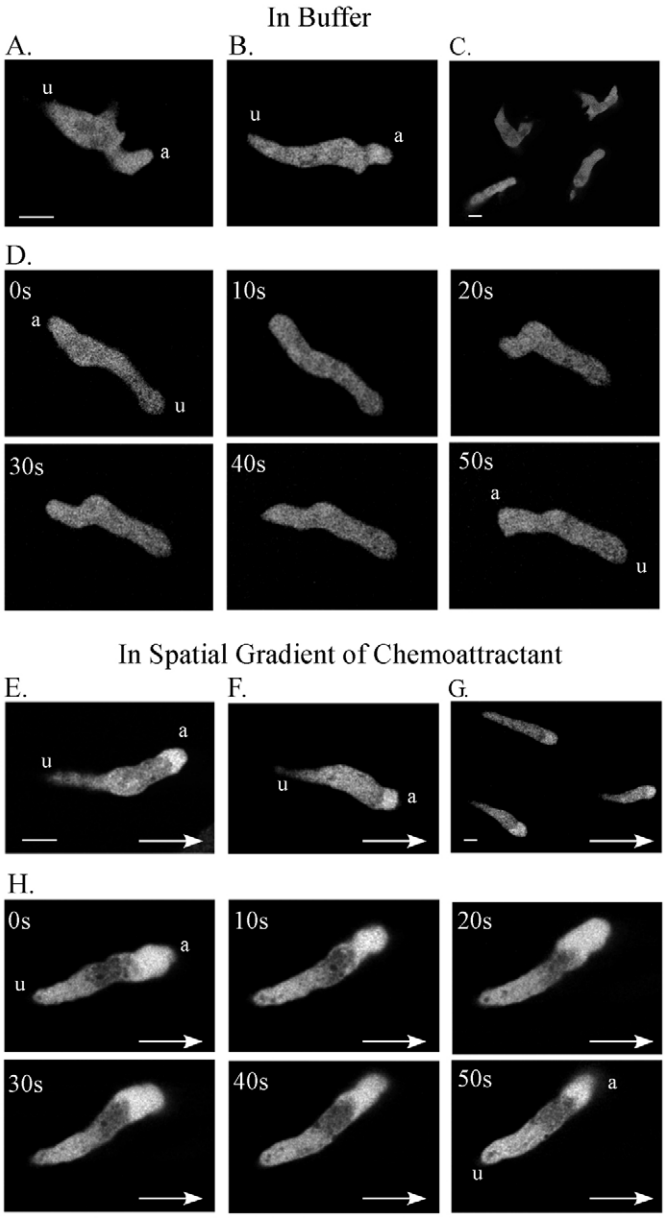

Fig. 3. The SBDS protein is distributed relatively evenly throughout the cytoplasm and pseudopod of *D. discoideum* amoebae that migrate in buffer, but is enriched in the anterior pseudopods of cells that undergo chemotaxis in a spatial gradient of chemoattractant. Cells carrying GFP-tagged SBDS were imaged with LSCM 1 μm above the substratum. (A,B,C) Examples of the even distribution of SBDS-GFP in cells that migrate in buffer. (D) Images of a single cell migrating in buffer, taken every 10 seconds and 1 μm above the substratum. (E,F,G) Examples of the enrichment of SBDS-GFP in the pseudopods of cells undergoing chemotaxis. (H) Images of a single cell undergoing chemotaxis, taken every 10 seconds and 1 μm above the substratum. Arrows represent the direction of increasing chemoattractant concentration; a, anterior end; u, uropod. Bars, 5 μm (bar in A also represents B, D; bar in E also represents F, H).

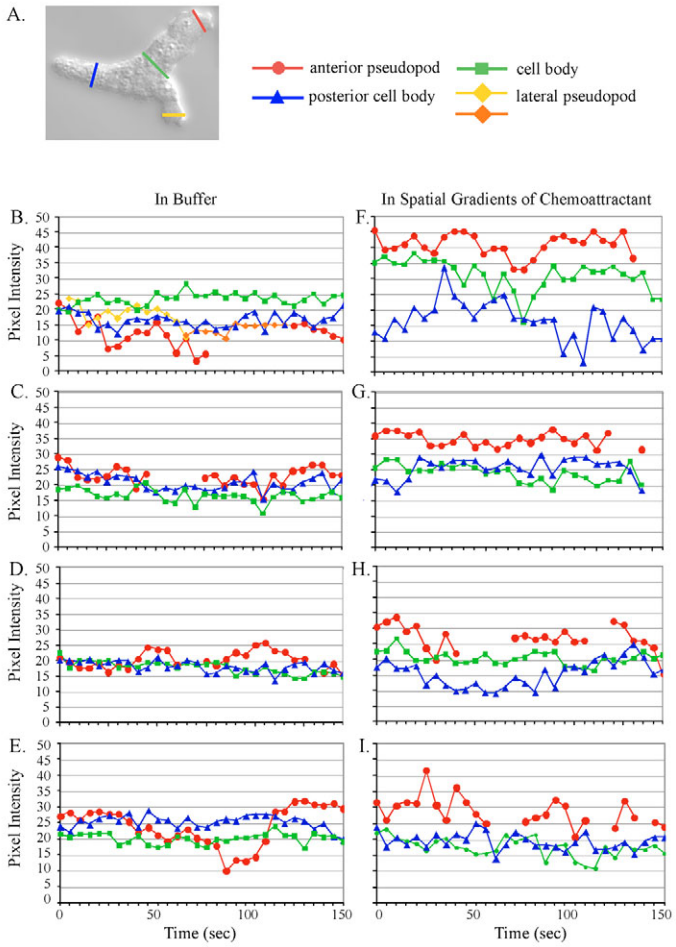

Fig. 4. Pixel intensity of line scans made with the LSCM across different parts of the cell. Each data point is the average of the line scan taken as the cell either migrates in buffer or undergoes chemotaxis. (A) Diagram of line scans and color code of different parts of cell body. (B-E) Examples of cells migrating in buffer. (F-I) Examples of cells undergoing chemotaxis in a spatial gradient of attractant. Notice that the average pixel intensity across pseudopods is similar to that of the cell body in buffer, but consistently higher in cells undergoing chemotaxis.

Journal of Cell Science

higher in pseudopods than in the main cell body (Fig. 3E-G; supplementary material Movie 1, panel B). The enrichment of SBDS in pseudopods of cells undergoing chemotaxis was observed in scans through the *z*-axis (data not shown). Localization in the pseudopod was stable, as is demonstrated in scans 1 μm off the substratum taken at short time intervals throughout a 50-second period (Fig. 3H). Average pixel-intensity measurements along line scans across pseudopodia were consistently higher than scans across the front or back of the cell body (Fig. 4F-I). The difference was relatively constant over the time period of analysis of each cell (150 sec). The ratio of average intensity across the pseudopod *versus* cell body for eight amoebae undergoing chemotaxis in a spatial gradient of chemoattractant was 1.50±0.26, compared with 1.07±0.14 for cells migrating in buffer (Table 1). The difference was significant (P=0.0033).

Localization of the SBDS protein to sites of lateral pseudopod formation

When a cell that underwent chemotaxis made a lateral pseudopod, the SBDS-GFP protein localized to the site very close to the time of initial protrusion (Fig. 5A, 80-110 seconds; supplementary material Movie 2, panel B). SBDS-GFP then remained localized in the expanding lateral pseudopod (Fig. 5A, 105-120 seconds; Fig. 5B, 10-40 seconds). Upon retraction, SBDS-GFP localization in the lateral pseudopod ended (Fig. 5A, 140 seconds; Fig. 5B, 55 and 65 seconds). SBDS-GFP remained localized in the dominant anterior pseudopod during lateral pseudopod expansion and retraction.

Localization of SBDS in response to attractant under non-gradient conditions

The preceding results clearly demonstrated that a spatial gradient of chemoattractant induced localization of SBDS-GFP in pseudopodia. We found, however, that cells in a spatial gradient of chemoattractant that were oriented in the direction of increasing attractant concentration (the majority) and cells that were oriented in the direction of decreasing attractant concentration (the minority) both showed SBDS-GFP enrichment in their anterior pseudopod, suggesting that not the gradient per se but simply receptor occupancy induced enrichment. To test this possibility, cells were perfused for 10 minutes with a constant concentration of chemoattractant (5×10^{-8} M cAMP) equal to that in the middle of the front of the wave, and then analyzed for SBDS localization by LSCM. Perfusion was performed in a round chamber at a high flow rate, conditions that excluded gradient formation. Whereas control cells perfused with buffer exhibited uniform SBDS-GFP distribution throughout the cytoplasm and pseudopods (Fig. 6A), cells perfused with chemoattractant exhibited SBDS-GFP enrichment in the pseudopod (Fig. 6B,C). However, enrichment was not stable like in spatial gradients. Over a 10-minute period in buffer, enrichment was transient, whereas over a 10-minute period in a spatial gradient, enrichment was persistent (data not shown).

Transformants with non-integrated copies of *SBDS-GFP*

To generate a non-integrating plasmid, the *D. discoideum SBDS* gene was inserted into the plasmid pTX-GFP in-frame with *GFP* (Levi et al., 2000). pTX-GFP contains the autonomously replicating element Dddp1 and the neomycin resistance gene, which confers G418 resistance (Liu et al., 2000). Five copies on average are carried by replicating cells (Nellen et al., 1984). A G418-resistant, GFP-expressing clone was selected and named GFP4-SBDS. This strain was analyzed with DIAS motion analysis software (Soll, 1995; Soll and Voss, 1998) for shape and motility parameters in buffer, and for shape, motility and chemotaxis parameters in a spatial gradient of attractant. The behavior of GFP4-SBDS was indistinguishable from that of the parent strain AX3, both in buffer and in spatial gradients of attractant (data not shown).

GFP4-SBDS cells were examined with LSCM and imaged at the same settings as clones AX3p2.1.2 and AX2p2.3.1. During perfusion with buffer, SBDS-GFP was present throughout the cytoplasm and pseudopods, with no enrichment in the cortex, pseudopod or uropod. This was true for more than 100 analyzed cells. The pseudopod:cell-body ratio of pixel intensities ranged between 0.90 and 1.1 for seven analyzed cells. Scans were again performed through a *z*-series and through a time series of 5 minutes. Persistent enrichment was not observed (data not shown).

In a spatial gradient of attractant, the majority of the GFP4-SBDS cells oriented towards the

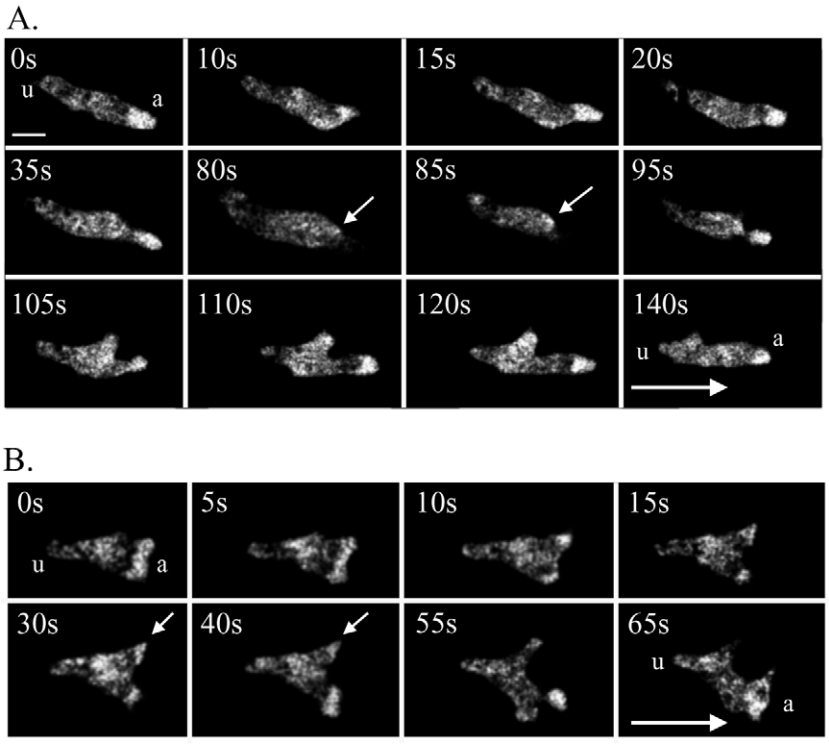

Fig. 5. SBDS-GFP localizes to the site of incipient lateral pseudopod formation, remains localized in the pseudopod during extension and exits the pseudopod upon retraction. (A,B) Two representative examples of localization. Small arrows point to SBDS-GFP localization in lateral pseudopods. Large arrows indicate direction of spatial gradients. Time is given in seconds (s); a, anterior end; u, uropod. Bar, 5 μm.

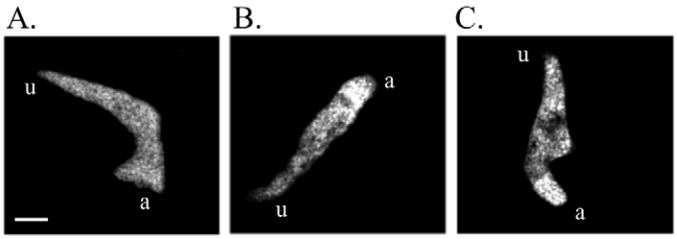

Fig. 6. SBDS-GFP localizes to the pseudopods of cells treated in a perfusion chamber with a constant concentration of chemoattractant (cAMP). (A,B) Cells were perfused before imaging with (A) buffer in the absence of cAMP for 10 minutes or (B,C) buffer containing 5×10^{-8} M cAMP for 10 minutes; a, anterior end; u, uropod. Bar, 5 μm.

cAMP source, extended fewer lateral pseudopods and turned less often than they did in buffer alone. Whereas SBDS-GFP was present throughout the cell, it was enriched in the pseudopod, with ratio measurements ranging from 1.35 to 1.5 for seven analyzed cells. When exposed to a constant concentration of 5×10^{-8} M cAMP for 10 minutes, enrichment of SBDS-GFP to anterior and lateral pseudopods was apparent (Fig. 6C). Therefore, SBDS protein localized to pseudopods in response to cAMP, regardless of an integrated or extrachromosomal *SBDS-GFP* gene.

Discussion

Our previous behavioral analysis of the PMNs of SBDS patients revealed a single defect (Stepanovic et al., 2004). Although cell polarization, basic cellular translocation and lateral pseudopod formation were normal in SBDS PMNs, the capacity to orient in a spatial gradient of the chemoattractant fMLP was lost. This was true for all tested SBDS patients, which was surprising, given that not all were expected to harbor mutations or exhibit changes in expression of the *SBDS* gene (Boocock et al., 2003; Savchenko et al., 2005). Because of the specific defect in chemotactic orientation, we hypothesized that the SBDS protein plays a direct role in chemotaxis in a spatial gradient of chemoattractant and, therefore, is enriched in the anterior pseudopod of a cell undergoing chemotaxis – as is the case for several key proteins involved in the regulation of chemotactic orientation (Postma et al., 2004; Van Haastert and Devreotes, 2004; Servant et al., 2000).

To test this hypothesis, we overexpressed *SBDS-GFP* in *D. discoideum*, a model system for animal cell chemotaxis, and demonstrated that the protein accumulated in pseudopods only when cells were treated with chemoattractant. This was true for transformants whose *SBDS-GFP* gene was ectopically integrated and for those whose gene was not integrated into the genome. Our results suggest that localization of SBDS to the pseudopod is a chemotactic response and not a result of polarization per se, because cells polarize and translocate in buffer in the absence of chemoattractant. This result is consistent with the single behavioral defect exhibited by SBDS PMNs in a spatial gradient of chemoattractant (Stepanovic et al., 2004). The behavioral defect of SBDS PMNs is expressed only under chemotactic conditions, as is the enrichment of the SBDS protein in pseudopods in *D. discoideum*.

It seemed likely from the structural, mutational and biochemical studies of SBDS that its major role is in RNA metabolism (Savchenko et al., 2005; Shammas et al., 2005). In the Archaea, the *SBDS* ortholog is harbored in an operon that contains genes encoding RNA-processing enzymes (Koonin et al., 2001), and in yeast it has been demonstrated that the *SBDS* ortholog is coexpressed with genes encoding RNA processing enzymes (Wu et al., 2002). In experiments in which the *S. cerevisiae* SBDS homolog YLR022C was TAP-tagged at its C-terminus and purified by tandem affinity-chromatography, several proteins involved in rRNA processing, including components of the 60S ribosomal particle, co-purified (Savchenko et al., 2005). Genetic and protein interaction studies (Savchenko et al., 2005) of YLR022C and the *S. cerevisiae* gene YHR087W, a distant homolog of YLR022C, revealed possible interactions with Np13, a protein which is involved in rRNA processing and nuclear export, and which is associated with the U1 small nuclear ribonucleoprotein particle (U1 snRNP) (Russell and Tollerwey, 1992; Singleton et al., 1995; Gottschalk et al., 1998) and Yra2, a protein associated with RNP complexes (Zenklusen et al., 2001; Inoue et al., 2000). The yeast YHR087W protein has been shown to interact with the SR protein kinase, which phosphorylates SR domains in splicing factors and regulates splicing, and also with ribosomal proteins, suggesting a role in the assembly of ribosomal particles (Ito et al., 2001; Uetz et al., 2000; Ho et al., 2002). Staining of normal fibroblasts with anti-SBDS antibody revealed diffuse cytoplasmic and nuclear staining, and enrichment in nucleoli (Austin et al., 2005), which is consistent with its role in rRNA metabolism. In addition, our analysis here revealed orthogonally placed SHHP motifs, which form a cleft that might serve as a surface for interactions with a ribonucleoprotein complex.

The localization of SBDS to the pseudopod in response to chemoattractant might seem counter-intuitive given the deduced role of SBDS in RNA metabolism and transport. However, SBDS might play a role in the translocation of molecules involved in the regulation of chemotaxis from the nucleus to the pseudopod (Devreotes and Janetopoulos, 2003; Merlot and Firtel, 2003; Postma et al., 2004; Van Haastert et al., 2004; Ridley et al., 2003), a premise that draws some credibility from observations of the localization of β-actin mRNA in pseudopodia (Sundell and Singer, 1990; Hill and Gunning, 1993; Kislauskis et al., 1994; Condeelis and Singer, 2005) and the localization of mRNAs of the seven proteins in the Arp2/3 complex in fibroblast projections stimulated by serum (Mingle et al., 2005). Although the number of polysomes in *Dictyostelium* declines with the initiation of development (Alton and Lodish, 1977), they do persist in association with significant levels of protein synthesis (Cardelli and Dimond, 1981). In addition, globular structures interpreted as ribosomes have been visualized by transmission electron microscopy (TEM) in the lamellipodia of mouse melanoma cells (Resch et al., 2005) and in pseudopods of starved *Dictyostelium* amoebae (D.R.S., unpublished data). Calculations of the rate of translation of β-actin mRNA reveal that in spite of the relatively small amount of message present in lamellipodia, its concentration at that site would make a significant difference in the amount of available protein (Condeelis and Singer, 2005).

In *D. discoideum*, phosphoinositol kinases that generate the

Journal of Cell Science

Journal of Cell Science

phosphatidylinositols PtdIns(4,5)P_2 or PtdIns(3,4,5)P_3 localize to the leading edge of cells responding to a spatial gradient of chemoattractant, whereas the tumor suppressor PTEN (a PI 3-kinase that removes these signaling molecules) is excluded and localizes in the cortex of the main cell body (Devreotes and Janetopoulos, 2003; Merlot and Firtel, 2003). It has been proposed that these enzymes are involved in an intracellular gradient-amplification mechanism for assessing and responding to spatial gradients of attractant (Janetopoulos et al., 2004; Ridley et al., 2003). This system appears to be involved in the regulation of lateral pseudopods, presumably through the Arp2/3 complex, which also localizes to the leading edge of pseudopods (Machesky and Insall, 1999; Pollard et al., 2000; Svitkina and Borisy, 1999; Welch et al., 1997). Several observations suggest that SBDS interacts with a subset of these signal transduction molecules. For example, screens of a yeast proteome microarray revealed that the SBDS yeast homolog binds strongly and specifically to phosphatidylinositol-tagged liposomes (Zhu et al., 2001). It also binds to Rho3p (Zhu et al., 2001), a GTPase involved in actin-filament organization, suggesting that SBDS either plays a role in linking the distribution of mRNAs with the dynamic rearrangement of the cytoskeleton, or is directly involved in cytoskeletal reorganization.

Our results indicate that the SBDS-GFP protein localizes to the site of protrusion very early in the process of pseudopod formation. We found that this was also the case for Scar, a WASP-related protein in *D. discoideum* (J. Steiner, D.W., D.R.S. and C. L. Saxe, unpublished observations) that associates with the Arp2/3 complex (Machesky and Insall, 1998; Suetsugu et al., 1999). However, unlike SBDS-GFP localization, Scar localizes to protrusions in the absence as well as in the presence of chemoattractant. Therefore, if the SBDS protein regulates the synthesis of a protein or proteins associated with the Arp2/3 complex or plays a role in pseudopod protrusion, it must do so only within the context of chemotaxis.

We have demonstrated that localization of SBDS to the pseudopod occurs in response to treatment with chemoattractant, and not only to gradient conditions. This is consistent with our observation that, SBDS localizes to the site of new lateral pseudopod formation – sometimes in the direction of decreasing chemoattractant concentration – and to the anterior pseudopod of the few cells oriented in the wrong direction of a spatial gradient of attractant. However, preliminary data indicate that the kinetics of pseudopod localization differ in constant concentrations versus gradient conditions (D.W. and D.R.S., unpublished observations). This observation is now being explored.

To demonstrate enrichment of the SBDS protein in pseudopodia in response to attractant, we employed transformed cells harboring multiple copies of the *SBDS-GFP* gene under the regulation of its own promoter, integrated ectopically or harbored in a non-integrating plasmid. The interpretations of localisation are open to the reservation that overexpressed proteins may nest in abnormal locations. This, however, seems implausible given that the protein localizes to pseudopods and to the site of incipient pseudopod formation only upon treatment with chemoattractant. Overexpression had no measurable effect on basic motile behavior or chemotaxis as assessed by computer-assisted methods. What is more, localization fits the prediction based upon the defect demonstrated in SBDS PMNs (Stepanovic et al., 2004).

Although the results of SBDS enrichment in pseudopods in *D. discoideum* are consistent with a role in human PMN chemotaxis (which was suggested by the defect observed in SBDS PMN chemotaxis) it is not immediately obvious that the results are consistent with the other multisystem defects of SBDS patients, such as pancreatic insufficiency and skeletal abnormalities. It is possible that they are, and that all of the abnormalities observed in SBDS patients result from a common defect in the regulation of signal-induced cellular protrusions. Identifying the proteins that interact with the SBDS protein in response to chemoattractant might reveal not only its role in chemotactic orientation but also a more general role in signal-induced cell behaviors other than that of PMNs. Our attempts to delete the *SBDS* gene in *D. discoideum* have been unsuccessful, suggesting that it is essential. Similarly, deletion of the *SBDS* ortholog in *S. cerevisiae* was lethal (Winzeler et al., 1999) as were some truncation mutations (Shammas et al., 2005). Gene-replacement studies in *D. discoideum* are underway that include the *SBDS* gene harboring mutations similar to those that have been identified in the *SBDS* gene of SBDS patients. In addition, immunoprecipitation experiments are in progress to identify SBDS-associated macromolecules, RNA and proteins in cAMP-treated and -untreated cells.

Materials and Methods

Culture conditions

Cultures of *D. discoideum* strains AX3, AX2 or GFP-tagged derivatives, were generated every 2 weeks by incubating glycerol stocks of spores in HL-5 medium (Cocucci and Sussman, 1970) for 2 days to induce germination. Amoebae were then transferred to fresh medium and grown to a final concentration of 2×10^6 cells/ml (Sussman, 1987). Amoebae were then washed in buffered salts solution (BSS; 20 mM KCl, 2.5 mM $MgCL_2$ and 20 mM KH_2PO_4, pH 6.4) (Sussman, 1987) and dispersed as a smooth carpet on a black filter pad saturated with BSS at a density of 5×10^6 per cm^2 (Soll, 1987). Cells were harvested after approximately 7 hours, at the onset of aggregation (Soll, 1979), washed and dispersed on the glass wall of a perfusion chamber for analysis in buffer, or on the bridge of a spatial gradient chamber for analysis in a gradient of chemoattractant.

Construction of the *Dictyostelium GFP-SBDS* chimeric in-frame fusion gene for integration

The *D. discoideum* homolog of SBDS (DDB0206557) was identified by a BLAST analysis of the human SBDS protein against the protein database in the *D. discoideum* genome project data base (http://dictybase.org/db/cgi-bin/blast.pl). A DNA fragment of 1202 nucleotides, beginning at bp –260 and ending at bp +942 relative to the start codon of the *D. discoideum* SBDS gene, was then amplified by high-fidelity polymerase chain reaction (PCR) (Roche Diagnostics, Indianapolis, IN) using the primer pairs SBDSF1 (5′-ATC AAA TAA TCT GAT TGA TC-3′) and SBDSR2 (5′-GGA CAA GAT ATA GGT ACA CCG-3′), and genomic DNA from *D. discoideum* strain AX3 as template. The PCR product was subcloned into the pGEM-Teasy plasmid vector (Promega Corp., Madison, WI) and the recombinant plasmid pDdSDS-2 selected and verified by sequencing of the inserted DNA. To generate the GFP-SBDS fusion, a *Sma*I restriction enzyme site was introduced at the 5′ end of the TAA stop codon of the SBDS coding region by inverse PCR, using primer pairs DSDgfIN3 (5′-TCG CCC GGG TTT TGA AGATGA AGT TGT GGT GG-3′) and DSDgfIN4 (5′-TCG CCC GGG AAA TAA ATA AAA AAA AAA AAA AAA AAA CAA ATT CCC-3′). The inverse PCR product was generated using the high-fidelity long PCR system (Roche Diagnostics, Indianapolis, IN) and digested with *Sma*I followed by ligation with a GFP-neomycin expression module. The 2710 bp GFP-neomycin module was generated with a high-fidelity long PCR system (Roche Diagnostics) using primer pairs gfnestuf1 (5′-TCG AGG CCT ATG TAT CAT CAT CAT CAT CAT CAT C-3′) and gnfestur1 (5′-TCG AGG CCT TCA AAA AGA TAA AGC TGA TCC-3′), and the plasmid pTX-GFP, kindly provided by Thomas T. Egelhoff (Case Western Reserve College of Medicine, Cleveland, OH) (Levi et al., 2000). The expression module was digested with *Stu*I and ligated into the *Sma*I site of the inverse PCR product to generate the GFP in-frame fusion at the C-terminal end of the *D. discoideum* SBDS protein. The derived plasmid was designated pSDGFNe2.1.

Journal of Cell Science

Directional cloning and in-frame fusion were verified by DNA sequencing. For transformation of *D. discoideum* amoebae, the SBDS-expression module was isolated by digestion of 25 μg of plasmid DNA with *Not*I. The digested plasmid DNA was cleaned using the QIAQUICK PCR Purification Kit (Quiagen Inc., Valenicia, CA) and eluted in 40 μl H_2O.

Construction of the *GFP-SBDS* chimeric in-frame fusion gene in an autonomously replicating plasmid

A DNA fragment of 1473 nucleotides, beginning at bp –531 and ending at bp +942 relative to the start codon of the *D. discoideum* SBDS gene, was amplified by high fidelity PCR using the primer pairs DSBPRF1 (5′-CGTGTCGACTTAGATTT-AAAATTTTTAAAC-3′) and DSBTPR2 (5′-CGTGGTACGATATCTTTTGAAG-ATGAAGTTGTGG-3′), and genomic DNA from *D. discoideum* strain AX3 as template. The PCR product was subcloned into the pGEM-T Easy vector (Promega Corp., Madison, WI), and the selected recombinant clone pYS-9.1 verified by sequencing. To generate the expression module, the plasmid was digested using the restriction enzymes SalI and KpnI. The *SBDS* gene fragment was purified from a 0.8% agarose gel using the QIAquick Gel Extraction Kit (QIAGEN Sciences, MD, USA), and ligated into dephosphorylated GFP-based plasmid pTX-GFP, a generous gift from Thomas T. Egelhoff (Levi et al., 2000). Two derived plasmids, pYS-13.1 and pYS-13.2, were verified for correct fusion by sequencing. For transformation of *D. discoideum* AX3 cells, plasmids pYS-13.1 and pYS-13.2 were purified through QIAprep Spin Miniprep Kit (QIAGEN Sciences, MD, USA).

Transformation and screening for GFP-expressing clones

Transformation was carried out according to the method of Pang et al., (Pang et al., 1999), with minor modifications. Approximately 5×10^6 cells were pelleted, washed twice in ice cold H-50 buffer (20 mM Hepes, 50 mM KCl, 10 mM NaCl, 1 mM $MgSO_4$, 5 mM $NaHCO_3$, and 1 mM NaH_2PO_4, pH 7.0), resuspended in 100 μl of H-50 buffer and mixed with 5 μl of the expression cassette containing 5-10 μg DNA. Electroporation was performed by pulsing the cells for 1 second, followed 5 seconds later by a second pulse, in a 0.1-cm cuvette in the cold at 0.85 kV/25 μF/ 200 Ω using a Gene Pulser (BioRad Labs, Inc. Hercules, CA). Cells were then incubated on ice for 5 minutes. Electroporated cells were recovered in 500 μl of HL-5 medium and transferred to 10-cm Petri dishes containing 10 ml of HL-5 medium. After 48 hours of incubation, G418 was added to a final concentration of 5 μg/ml. After 4-5 days, G418-resistant transformants were clonally selected by diluting approximately 100 cells into 500 μl of a suspension of the bacterium *Klebsiella aerogenes* and spreading the mixture onto a 15-cm slime mold agar plate (Sussman, 1966). Plates were incubated for 3-4 days at 22°C until plaques arose from single amoebae feeding on the bacteria. Cells from each plaque (clone) were picked and transferred back into individual 10-cm Petri plates containing 10 ml of HL-5 medium supplemented with 5 μg/ml G418. Cells in each plate were examined through a Zeiss Axiovert 100 fluorescence microscope (Zeiss, Inc., Thornwood, NY) and those clones in which 100% of the cells were fluorescent were chosen.

PCR analysis

For PCR analysis of integrated SBDS expression modules, 10^8 cells were pelleted and resuspended in 0.5 ml of a solution containing 20 mM Tris-HCl pH 7.6, 5 mM magnesium acetate, 0.5 M EDTA and 5% sucrose. Cells were lysed and intact nuclei released by adding 0.2 ml of 10% Triton-X 100 and incubating the mixture on ice for 5 min (Levi et al., 2000). Nuclei were pelleted by centrifugation at 12,000 ***g*** for 5 min at room temperature. The pellet was resuspended in 0.3 ml of a solution containing 100 mM Tris-HCL, pH 7.5, 5 mM EDTA, 100 μg/ml proteinase K and 1% SDS, extracted with 150 μl of a 1:1 mixture of Tris-buffered phenol:chloroform, and nucleic acids precipitated by addition of 2.5 volumes of 100% ethanol. The precipitated nucleic acids were pelleted by centrifugation, dried, resuspended in 50 μl of water and treated with 0.5 μl RNaseA (10 μg/ml) for 60 min at 37°C. This preparation was further diluted 1:100 for use in PCR reactions. To test the integrity of the expression module, the primer pairs SBDSF1 and DdgfSq1 (5′-GGG TAA GTT TTC CGT ATG TTG C-3′) were employed. PCR amplification was performed with Taq polymerase (New England Biolabs, Beverly, MA). The protocol was 1 minute of denaturation at 92°C, 1 minute of annealing at 42°C and 2 minutes of extension at 68°C, for 40 cycles.

Southern and northern analyses

Southern and northern analyses were performed according to methods previously described (Lachke et al., 2000; Srikantha et al., 2000; Srikantha et al., 2001). Total RNA for northerns was prepared by the RNeasy kit as recommended by the manufacturer (QIAGEN, Valencia, CA). Southern and northern blots were quantitated by digitizing images of blots into DENDRON software (Srikantha et al., 2002) and quantitating pixel density against standards plots (Srikantha et al., 2000).

Analysis of cell behavior in buffer and in a spatial gradient of cAMP

The methods for analyzing single cells migrating in buffer under perfusion conditions are described in detail elsewhere (Wessels et al., 2000b; Zhang et al., 2002; Zhang et al., 2003). In brief, cells were distributed on the glass surface of a Sykes-Moore perfusion chamber (Bellco Glass, Vineland, NJ) and positioned on the stage of a Nikon TE2000 microscope in a BioRad Radiance 2100MP laser scanning confocal microscope (LSCM) system. The chamber was perfused with buffered salts solution at a rate that prevented conditioning of the soluble microenvironment. The methods for analyzing single cells undergoing chemotaxis in a spatial gradient of the chemoattractant cAMP have also been described in detail elsewhere (Shutt et al., 1998; Wessels et al., 2000; Zhang et al., 2002; Zhang et al., 2003; Varnum-Finney et al., 1987b). The quartz chamber, described in detail by Shutt et al. (Shutt et al., 1998), supported cells on a bridge bordered by two troughs, one containing buffer alone and one containing buffer plus 10^{-6} M cAMP. Cells were analyzed by LSCM after 10 minutes of incubation.

Fluorescence imaging and quantitative analysis

Live cells migrating in buffer or in a spatial gradient of cAMP were examined by LSCM using the 60× plan apochromat water immersion objective (numerical aperture 1.2) and a 2.6× digital zoom. LaserSharp 2000 (release 5.2) software was used for image acquisition. GFP was excited using the 488 nm argon laser line at 15% power. Simultaneous differential interference contrast (DIC) images were generated using the 476 nm argon laser at 10% power. Acquisition parameters were set by imaging a cell in buffer with uniform fluorescence distribution. The grayscale dynamic was optimized using the set col.lut lookup table to eliminate pixel saturation and to ensure that pixel intensity was linear and that the full dynamic range from 0 to 255 of the 8-bit photomultiplier detector was utilized. Once these parameters were set, the software was unchanged for all subsequent image acquisition. Sixty frames of a crawling cell were collected at 5-second intervals in an *xy* time series at a scan rate of 166 lines per second without frame averaging. The stored frames were subsequently exported into TIFF format using LaserSharp 2000 software. The TIFF series was then imported into Quick Time Pro 7™ and saved as a movie. The Quick Time movie was opened in DIAS 3.4.1™ (Soll Technologies, Inc., Iowa City, IA) and pixel intensity measured as a line profile across the pseudopod or cell body. These data were opened in Microsoft Excel™ software for plotting relative intensity and pixel intensity ratios of pseudopod to cell body. Confocal images were exported to Adobe Photoshop™ for manuscript preparation.

Bioinformatic analysis of SBDS

The nonredundant (NR) database of protein sequences (National Center for Biotechnology Information, NIH, Bethesda) was searched using the BLASTP program (Altschul et al., 1990). Iterative database searchers were conducted using the PSI-BLAST program with either a single sequence or an alignment used as the query, with the PSSM inclusion expectation (E) value threshold of 0.01; the searchers were iterated until convergence (Altschul et al., 1997). Multiple alignments were constructed using the MUSCLE program (Edgar et al., 2004), followed by manual correction based on the PSI-BLAST results. Protein secondary structure was predicted by using a multiple alignment to generate an HMM and PSSM, which were then used by the Jpred program to produce a final structural prediction with 72% accuracy or more (Cuff et al., 1998). Protein-structure manipulations were performed using the Swiss-PDB viewer program and ribbon diagrams were constructed using the PYMOL program (Guex and Peitsch, 1997).

This research was funded by a grant from Shwachman-Diamond Syndrome International and by grant HD-18577 from the National Institutes of Health.

References

Aggett, P., Cavanagh, N., Matthew, D., Pincott, J., Satcliff, J. and Harris, J. (1980). Shwachman's syndrome: a review of 21 cases. *Arch. Dis. Child.* **55**, 331-347.

Alton, T. and Lodish, H. (1977). Translation control of protein synthesis during the early stages of differentiation of the slime mold *Dictyostelium discoideum*. *Cell* **12**, 301-310.

Altschul, S. F., Gish, W., Miller, W., Myers, E. W. and Lippman, D. J. (1990). Basic local alignment search tool. *J. Mol. Biol.* **215**, 403-410.

Altschul, S. F., Madden., T. L., Schaffer, A. A., Zhang, J., Zhang, Z., Miller, W. and Lipman, D. J. (1997). Gapped BLAST and PSI-BLAST: a new generation of protein database search programs. *Nucleic Acids Res.* **25**, 3389-3402.

Austin, K., Leary, R. and Shimamura, L. (2005). The Shwachman-Diamond SBDS protein localizes to the nucleolus. *Blood*. 106, 1253-1258.

Bodian, M., Sheldon, W. and Lightwod, R. (1964). Congenital hypoplasia of the exocrine pancreas. *Acta Paediatr.* **53**, 282-293.

Boocock, G., Morrison, J., Popovic, M., Richards, N., Ellis, L., Durie, P. and Rommens, J. (2003). Mutations in SBDS are associated with Shwachman-Diamond Syndrome. *Nat. Gen.* **33**, 97-101.

Cardelli, J. and Dimond, R. (1981). Regulation of protein synthesis in *Dictyostelium discoideum*: effects of starvation and anoxia on initiation. *Biochemistry* **20**, 7391-7398.

Chung, C., Potikyan, G. and Firtel, R. (2001). Control of cell polarity and chemotaxis by Akt/PKB and PI3 kinase through the regulation of PAKa. *Mol. Cell* **7**, 937-947.

Cipolli, M., D'Orazio, C., Delmarco, A., Marchesini, C., Miano, A. and Mastella, G. (1999). Shwachman's syndrome: pathomorphosis and long-tern outcome. *J. Pediatr. Gastroenterol. Nutr*. **29**, 265-272.

Coccuci, S. and Sussman, M. (1970). RNA in cytoplasmic and nuclear fractions of cellular slime mold amebas. *J. Cell Biol.* **45**, 399-407.
Condeelis, J. and Singer, R. (2005). How and why does beta-actin mRNA target? *Biol. Cell* **97**, 97-110.
Cuff, J. A., Clamp, M. E., Siddiqui, A. S., Finlay, M. and Barton, G. J. (1998). JPred: a consensus secondary structure prediction server. *BioInformatics* **14**, 892-893.
Devreotes, P. and Janetopoulos, C. (2003). Eukaryotic chemotaxis: distinctions between directional sensing and polarization. *J. Biol. Chem.* **278**, 20445-20448.
Dror, Y., Ginzberg, H. and Dalal, I., Cherepanov, V., Downey, G., Durie, P., Roifman, C. and Freedman, M. (2001). Immune function in patients with Shwachman-Diamond syndrome. *Br. J. Haematol.* **114**, 712-718.
Edgar, R. C. (2004). MUSCLE: a multiple sequence alignment method with reduced time and space complexity. *BMC Bioinformatics* **5**, 113.
Funamoto, S., Milan, K., Meili, R. and Firtel, R. (2001). Role of phosphatidylinositol 3′ kinase and a downstream pleckstrin homology domain-containing protein in controlling chemotaxis in *Dictyostelium*. *J. Cell Biol.* **153**, 795-810.
Geiger, J., Wessels, D. and Soll, D. R. (2003). Human polymorphonuclear leukocytes respond to waves of chemoattractant, like *Dictyostelium*. *Cell Motil. Cytoskeleton* **56**, 27-44.
Ginzberg, H., Shin, J., Ellis, L., Morrison, J., Ip, W., Dror, Y., Freedman, M., Heitlinger, L., Belt, M., Corey, M., Rommens, J. and Durie, P. (1999). Shwachman syndrome: phenotypic manifestations of sibling sets and isolated cases in a large patient cohort are similar. *J. Pediatr.* **185**, 81-88.
Gottschalk, A., Tang, J., Puig, O., Salgado, J., Neubauer, G., Colot, H., Mann, M., Seraphin, B., Rosbash, M. et al. (1998). A comprehensive biochemical and genetic analysis of the yeast snRNP reveals five novel proteins. *RNA* **4**, 374-393.
Guex, N. and Peitsch, M. C. (1997). SWISS-MODEL and the Swiss-PdbViewer: an environment for comparative protein modeling. *Electrophoresis* **18**, 2714-2723.
Haugh, J., Codazzi, F., Teruel, M. and Meyer, T. (2000). Spatial sensing in fibroblasts mediated by 3′ phosphoinositides. *J. Cell Biol.* **151**, 1269-1280.
Hill, M. A. and Gunning, P. (1993). beta- and gamma-actin mRNAs are differentially located within myoblasts. *J. Cell Biol.* **122**, 825-832.
Ho, Y., Gruhler, A., Heilbut, A., Bader, G. D., Moore, L., Adams, S. L., Millar, A., Taylor, P., Bennett, K., Boutilier, K. et al. (2002). Systematic identification of protein complexes in *Saccharomyces cerevisiae* by mass spectrometry. *Nature* **415**, 123-124.
Inoue, K., Mizuno, T., Wada, K. and Hagiwara, M. (2000). Novel RING finger proteins, Air1p and Air2p, interact with Hmt1p and inhibit the arginine methylation of Npl3p. *J. Biol. Chem.* **275**, 32793-32799.
Insall, R., Taubenberger, A., Machesky, L., Kohler, J., Simmeth, E., Atkinson, S., Weber, I. and Gerisch, G. (2001). Dynamics of the *Dictyostelium* Arp2/3 complex in endocytosis, cytokinesis, and chemotaxis. *Cell Motil. Cytoskeleton* **50**, 115-128.
Ito, T., Chiba, T., Ozawa, R., Yoshida, M., Hattori, M. and Sakaki, Y. (2001). A comprehensive two-hybrid analysis to explore the yeast protein interactome. *Proc. Natl. Acad. Sci. USA* **98**, 4569-4574.
Janetopoulos, C., Ma, L., Devreotes, P. and Iglesias, P. (2004). Chemoattractant-induced phosphatidylinositol 3,4,5-triphosphate accumulation is spatially amplified and adapts, independent of the actin cytoskeleton. *PNAS* **101**, 8951-8956.
Jin, T., Zhang, N., Long, Y., Parent, C. and Devreotes, P. (2000). Localization of the G protein betagamma complex in living cells during chemotaxis. *Science* **287**, 1034-1036.
Kessin, R. H. (2001). *Dictyostelium*. Cambridge: Cambridge University Press.
Kislauskis, E. H., Zhy, X. and Singer, R. (1994). Sequences responsible for intracellular localization of beta-actin messenger RNA also affect cell phenotype. *J. Cell Biol.* **127**, 441-451.
Koonin, E., Wolf, Y. and Aravind, L. (2001). Prediction of the archael exosome and its connections with the proteasome and the translation and transcription machineries by a comparative-genomic approach. *Genome Res.* **11**, 240-252.
Kuijpers, T., Alders, M., Tool, A., Melliink, C., Roos, D. and Hennekan, R. (2005). Hematological abnormalities in Shwachman Diamond syndrome: lack of genotype-phenotype relationship. *Blood* **106**, 356-361.
Kuspa, A. and Loomis, W. F. (1994). REMI-RFLP mapping in the *Dictyostelium* genome. *Genetics* **138**, 665-674.
Lachke, S. A., Srikantha, T., Tsai, L., Daniels, K. and Soll, D. R. (2000). Phenotypic switching in *Candida glabrata* involves phase-specific regulation of the metallotheionein gene *MT-II* and the newly discovered hemolysin gene *HLP*. *Infect. Immun.* **68**, 884-895.
Levi, S., Polyakov, M. and Egelhoff, T. (2000). Green fluorescent protein and epitope tag fusion vectors for *Dictyostelium discoideum*. *Plasmid* **44**, 231-238.
Liu, X., Kohji, I., Lee, R. and Uyeda, T. (2000). Involvement of tail domains in regulation of *Dictyostelium* myosin II. *Biochem. Biophys. Res. Commun.* **271**, 75-81.
Machesky, L. and Insall, R. (1999). Signaling to actin dynamics. *J. Cell Biol.* **146**, 267-272.
Mack, D., Forstner, G., Wilschanski, M., Freedman, M. and Durie, P. (1996). Shwachman syndrome: exocrine pancreatic dysfunction and variable phenotypic expression. *Gastroenterology* **111**, 1593-1602.
Maffucci, T. and Falasca, M. (2001). Specificity in pleckstrin homology (PH) domain membrane targeting: a role for phosphoinositide-protein co-operative mechanism. *FEBS Lett.* **506**, 173-179.
Makitie, O., Ellis, L., Durie, P. R., Morrison, J., Sochett, E., Rommens, J. and Cole, W. (2004). Skeletal phenotype in patients with Shwachman-Diamond syndrome and mutations in SBDS. *Clin. Genet.* **65**, 101-112.
Meili, R., Ellsworth, C., Lee, S., Reddy, T., Ma, H. and Firtel, R. (1999). Chemoattractant-mediated transient activation and membrane localization of Akt/PKB is required for efficient chemotaxis to cAMP in *Dictyostelium*. *EMBO J.* **18**, 2092-2105.
Merlot, S. and Firtel, R. (2003). Leading the way: directional sensing through phosphatidylinositol 3-kinase and other signaling pathways. *J. Cell Sci.* **116**, 3471-3478.
Mingle, L., Okuhama, N., Shi, J., Singer, R., Condeelis, J. and Liu, G. (2005). Localization of all seven messenger RNAs for the actin–polymerization nucleator Arp2/3 complex in the protrusions of fibroblasts. *J. Cell Sci.* **118**, 2425-2433.
Nakashima, E., Mabuchi, A., Makita, Y., Masuno, M., Ohashi, H., Nishimura, T. and Ikegawa, S. (2004). Novel SBDS mutations caused by gene conversion in Japanese patients with Shwachman-Diamond syndrome. *Hum. Genet.* **114**, 345-348.
Nellen, W., Silan, C. and Firtel, R. A. (1984). DNA-mediated transformation in *Dictyostelium discoideum*: regulated expression of an actin gene fusion. *Mol. Cell Biol.* **4**, 2890-2898.
Pang, K., Lynes, M. and Knecht, D. (1999). Variables controlling the expression level of exogenous genes in *Dictyostelium*. *Plasmid* **41**, 187-197.
Parent, C. (2004). Making all the right moves: chemotaxis in neutrophils and *Dictyostelium*. *Curr. Opin. Cell Biol.* **16**, 14-23.
Parent, C., Blacklock, B., Froelich, W., Murphy, D. and Devreotes, P. (1998). G protein coupled signaling events are activated at the leading edge of chemotactic cells. *Cell* **95**, 81-91.
Pollard, T., Blanchoin, L. and Mullins, R. (2000). Molecular mechanisms controlling actin filament dynamics in nonmuscle cells. *Annu. Rev. Biophys. Biomol. Struct.* **29**, 545-576.
Postma, M., Bosgraaf, L., Loovers, H. and Van Haastert, P. (2004). Chemotaxis: signalling modules join hands at front and tail. *EMBO J.* **5**, 35-40.
Repo, H., Savilahti, E. and Leirisalo-Repo, M. (1987). Aberrant phagocyte function in Shwachman syndrome. *Clin. Exp. Immunol.* **69**, 204-212.
Resch, G., Goldie, K., Krebs, A., Hoenger, A. and Small, J. V. (2002). Visualisation of the actin cytoskeleton by cryo-electron microscopy. *J. Cell Sci.* **115**, 1877-1882.
Ridley, A., Schwartz, M., Burridge, K., Firtel, R., Ginsberg, M., Borisy, G., Parsons, J. and Horwitz, A. (2003). Cell migration: integrating signals from front to back. *Science* **302**, 1704-1709.
Rivero, F. and Somesh, B. (2002). Signal transduction pathways regulated by Rho GTPases in *Dictyostelium*. *JMRCM* **23**, 737-749.
Russell, I. and Tollervey, D. (1992). NOP3 is an essential yeast protein which is required for pre-rRNA processing. *J. Cell Biol.* **119**, 737-747.
Ruuter, P., Savilahti, E., Repo, H. and Kosunen, T. (1984). Constant defect in neutrophil locomotion but with age decreasing susceptibility to infection in Shwachman syndrome. *Clin. Exp. Immunol.* **57**, 249-255.
Savchenko, A., Krogan, N., Cort, J., Evdokimova, E., Lew, J., Yee, A., Sanchez-Pulido, L., Andrade, M., Bochkarev, A., Watson, J. et al. (2005). The Shwachman-Bodian-Diamond Syndrome protein family is involved in RNA metabolism. *J. Biol. Chem.* **280**, 19213-19220.
Servant, G., Weiner, O., Herzmark, P., Balla, T., Sedat, J. and Bourne, H. (2000). Polarization of chemoattractant receptor signaling during neutrophil chemotaxis. *Science* **287**, 1037-1040.
Shammas, C., Menne, T., Hilcenko, C., Michell, S., Goyenechea, B., Boocock, G., Durie, P., Rommens, J. and Warren, A. (2005). Structural and mutational analysis of the SBDS protein family: insight into the leukemia-associated Shwachman-Diamond syndrome. *J. Biol. Chem.* **280**, 19221-19229.
Shutt, D. C., Jenkins, L. M., Carolan, E., Stapleton, J., Daniels, K., Kennedy, R. and Soll, D. R. (1998). T cell syncytia induced by HIV release T cell chemoattractants: demonstration with a newly developed single cell chemotaxis chamber. *J. Cell Sci.* **111**, 99-109.
Shwachman, H., Diamond, L., Oski, F. and Khaw, K. (1964). The syndrome of pancreatic insufficiency and bone marrow dysfunction. *J. Pediatr.* **65**, 645-663.
Singleton, D., Chen, S., Hitomi, M., Kumagai, C. and Tartakoff, A. (1995). A yeast protein that bidirectionally affects nucleocytoplasmic transport. *J. Cell Sci.* **108**, 265-272.
Soll, D. R. (1979). Timers in developing systems. *Science* **203**, 841-849.
Soll, D. R. (1987). Gene expression and the opposing programs of differentiation and dedifferentiation in *Dictyostelium discoideum*. In *Advances in Gene Technology: The Molecular Biology of Development. Proceedings of 19th Miami Winter Symposium, ICSU Short Reports.* Vol. **7**, pp. 132-133. Miami: Miami Winter Symposium.
Soll, D. R. (1995). The use of computers in understanding how animal cells crawl. *Int. Rev. Cytol.* **163**, 43-104.
Soll, D. R. and Voss, E. (1998). Two and three dimensional computer systems for analyzing how cells crawl. In *Motion Analysis of Living Cells* (ed. D. R. Soll and D. Wessels), pp. 25-52. New York: John Wiley.
Soll, D. R., Wessels, D., Voss, E. and Johnson, O. (2001). Computer-assisted systems for the analysis of amoeboid cell motility. In *Methods in Molecular Biology: Cytoskeleton Methods and Protocols* (ed. R. H. Gavin), pp. 45-58. Totowa (NJ): Humana Press.
Soll, D. R., Wessels, D., Zhang, H. and Heid, P. (2002). A contextual framework for interpreting the roles of proteins in motility and chemotaxis in *Dictyostelium discoideum*. *J. Musc. Res. Cell Motil.* **23**, 659-672.
Srikantha, T., Tsai, L., Daniels, K. and Soll, D. R. (2000). *EFG1* null mutants of *Candida albicans* switch but cannot express the complete phenotype of white-phase budding cells. *J. Bacteriol.* **182**, 1580-1591.
Srikantha, T., Tsai, L. K., Klar, A. and Soll, D. R. (2002). The histone deacetylase

Journal of Cell Science

genes *HDA1* and *RPD3* play distinct roles in the regulation of high frequency phenotypic switching in *Candida albicans*. *J. Bacteriol*. **183**, 4614-4625.

Stepanovic, V., Wessels, D., Goldman, G., Geiger, J. and Soll, D. R. (2004). The chemotaxis defect of Shwachman-Diamond Syndrome Leukocytes. *Cell Motil. Cytoskeleton* **57**, 158-174.

Stepanovic, V., Wessels, D., Loomis, W. F. and Soll, D. R. (2005). Adenylyl cyclase plays an intracellular role in the suppression of lateral pseudopod formation during *Dictyostelium* chemotaxis. *Eukaryot. Cell* **4**, 775-786.

Suetsugu, S., Miki, H. and Takenawa, T. (1999). Identification of two human WAVE/SCAR homologues as general actin regulatory molecules which associate with the Arp2/3 complex. *Biochem. Biophys. Res. Commun.* **24**, 296-302.

Sundell, C. and Singer, R. (1990). Actin mRNA localizes in the absence of protein synthesis. *J. Cell Biol*. **111**, 2397-2403.

Sussman, M. (1966). *Methods in Cell Physiology* (ed. D.M. Prescott), p. 397. New York: Academic Press.

Sussman, M. (1987). Cultivation and synchronous morphogenesis of Dictyostelium under controlled experimental conditions. *Methods Cell Biol*. **28**, 9-29.

Svitkina, T. and Borisy, G. (1992). Arp2/3 complex and actin depolymerizing factor/cofilin in dendritic organization and treadmilling of actin filament array in lamellipodia. *J. Cell Biol.* **145**, 1009-1026.

Uetz, P., Giot, L., Cagney, G., Mansfield, T. A., Judson, R. S., Knight, J. R., Lockshon, D., Narayan, V., Srinivasan, M., Pochart, P. et al. (2000). A comprehensive analysis of protein-protein interactions in *Saccharomyces cerevisiae*. *Nature* **403**, 623-627.

Van Haastert, P. and Devreotes, P. (2004). Chemotaxis: signaling the way forward. *Nat. Rev*. **5**, 626-634.

Varnum-Finney, B., Edwards, K., Voss, E. and Soll, D. R. (1987a). Amoebae of *Dictyostelium discoideum* respond to an increasing temporal gradient of the chemoattractant cAMP with a reduced frequency of turning: evidence for a temporal mechanism in amoeboid chemotaxis. *Cell Motil. Cytoskeleton* **8**, 7-17.

Varnum-Finney, B., Voss, E. and Soll, D. R. (1987b). Frequency and orientation of pseudopod formation of *Dictyostelium discoideum* amoebae chemotaxing in a spatial gradient: Further evidence for a temporal mechanism. *Cell Motil. Cytoskeleton* **8**, 18-26.

Welch, M., DePace, A., Verma, S., Iwamatsu, A. and Mitchison, T. (1997). The human Arp2/3 complex is composed of evolutionarily conserved subunits and is localized to cellular regions of dynamic actin filament assembly. *J. Cell Biol.* **138**, 375-384.

Wessels, D., Reynolds, J., Johnson, O., Voss, E., Burns, R., Daniels, K., Garrard, E., O'Hallaran, T. and Soll, D. R. (2000). Clathrin plays a novel role in the regulation of cell polarity, pseudopod formation, uropod stability and motility in *Dictyostelium. J. Cell Sci.* **113**, 26-36.

Winzeler, E., Shoemaker, D., Astromoff, A., Liang, H., Anderson, K., Andre, B., Bangham, R., Benito, R., Boeke, J., Bussey, H. et al. (1999). Functional characterization of the S. cerevisiae genome by gene deletion and parallel analysis. *Science* **285**, 901-905.

Wu, L., Hughes, T., Davierwala, A., Robinson, M., Stoughton, R. and Altschuler, S. (2002). Large-scale prediction of *Saccharomyces cerevisiae* gene function using overlapping transcriptional clusters. *Nat. Genet*. **31**, 255-265.

Zenklusen, D., Vinciguerra, P., Strahm, Y. and Stutz, F. (2001). The yeast hnRNP-like proteins Yra1p and Yra2p participate in mRNA export through interaction with Mex67p. *Mol. Cell. Biol*. **21**, 4219-4232.

Zhang, H., Wessels, D., Fey, P., Daniels, K., Chisholm, R. and Soll, D. R. (2002). Phosphorylation of the myosin regulatory light chain plays a role in cell motility and polarity during *Dictyostelium* chemotaxis. *J. Cell Sci.* **115**, 1733-1747.

Zhang, H., Heid, P., Wessels, D., Daniels, K., Pham, T., Loomis, W. F. and Soll, D. R. (2003). Constitutively active protein kinase A disrupts motility and chemotaxis in *Dictyostelium discoideum*. *Eukaryot. Cell* **2**, 62-75.

Zhu, H., Belgin, M., Bangham, R., Hall, D., Casamayor, A., Bertone, P., Lan, N., Jansen, R., Bidlingmaier, S., Houfek, T. et al. (2001). Global analysis of protein activities using proteome chips. *Science* **293**, 2101-2105.

Zohn, I., Campbell, S., Khosravie-Far, R., Rossman, K. and Der, C. (1998). Rho family proteins and ras transformation: the RHOad less traveled gets congested. *Oncogene* **17**, 1415-1438.

Journal of Cell Science